

Research Article

Progesterone receptor membrane component 1 and 2 regulate granulosa cell mitosis and survival through a NF κ B-dependent mechanism[†]

John J. Peluso ^{1,2,*}, Cindy A. Pru ³, Xiufang Liu¹, Nicole C. Kelp³
and James K. Pru³

¹Department of Cell Biology, University of Connecticut Health Center, Farmington, Connecticut, USA; ²Department of and Obstetrics and Gynecology, University of Connecticut Health Center, Farmington, Connecticut, USA and ³Department of Animal Sciences, Center for Reproductive Biology, Washington State University, Pullman, Washington, USA

***Correspondence:** Department of Cell Biology (MC 3505), University of Connecticut Health Center, 263 Farmington Ave, Farmington, CT 06030, USA. E-mail: Peluso@UCHC.edu

[†]**Grant Support:** This work was supported by the following grants, NIH HD086402 and OD016564 as well as funding from the Department of Cell Biology, University of CT Health Center.

Edited by Dr. Jodi Flaws

Received 29 November 2018; Revised 13 February 2019; Accepted 15 March 2019

Abstract

Progesterone receptor membrane component 1 (PGRMC1) interacts with PGRMC2, and disrupting this interaction in spontaneously immortalized granulosa cells (SIGCS) leads to an inappropriate entry into the cell cycle, mitotic arrest, and ultimately cell death. The present study revealed that PGRMC1 and PGRMC2 localize to the cytoplasm of murine granulosa cells of nonatretic follicles with their staining intensity being somewhat diminished in granulosa cells of atretic follicles. Compared to controls (*Pgrmc1^{fl/fl}*), the rate at which granulosa cells entered the cell cycle increased in nonatretic and atretic follicles of mice in which *Pgrmc1* was conditionally deleted (*Pgrmc1^{Δ/d}*) from granulosa cells. This increased rate of entry into the cell cycle was associated with a ≥ 2 -fold increase in follicular atresia and the nuclear localization of nuclear factor-kappa-B transcription factor P65; (NF κ B/p65, or RELA). GTPase activating protein binding protein 2 (G3BP2) binds NF κ B/p65 through an interaction with NF κ B inhibitor alpha ($I\kappa$ B α), thereby maintaining NF κ B/p65's cytoplasmic localization and restricting its transcriptional activity. Since PGRMC1 and PGRMC2 bind G3BP2, studies were designed to assess the functional relationship between PGRMC1, PGRMC2, and NF κ B/p65 in SIGCs. In these studies, disrupting the interaction between PGRMC1 and PGRMC2 increased the nuclear localization of NF κ B/p65, and depleting PGRMC1, PGRMC2, or G3BP2 increased NF κ B transcriptional activity and the progression into the cell cycle. Taken together, these studies suggest that PGRMC1 and 2 regulate granulosa cell cycle entry in follicles by precisely controlling the localization and thereby the transcriptional activity of NF κ B/p65.

Summary Sentence

PGRMC1 and 2 regulates granulosa cell mitosis.

Key words: granulosa cell, mitosis, apoptosis, follicular development, ovary.

Introduction

Altered expression of either *Pgrmc1* [1] or *Pgrmc2* [2] is associated with a poor response to gonadotropin-induced follicle development in women undergoing in vitro fertilization as part their infertility treatment. Similarly, reduced expression of PGRMC1 due to either point and depletion mutations is correlated with primary ovarian insufficiency (POI) [3]. How these PGRMC family members affect follicle development in women is not known. However, it is known that conditional deletion of *Pgrmc1* interferes with the development of antral follicles in mice, thereby providing direct evidence that PGRMC1 plays an important role in antral follicle development [4].

In vitro studies using human granulosa/luteal cells [5, 6] or spontaneously immortalized granulosa cells (SIGCs) [7, 8] demonstrate that PGRMC1 and 2 regulate mitosis and apoptosis in part by suppressing the rate at which cells enter the cell cycle. Moreover, PGRMC1 complexes with PGRMC2 and depleting either *Pgrmc1* or *Pgrmc2* by siRNA treatment or disrupting their interaction with a PGRMC2 antibody initiates an inappropriate entry into the cell cycle, often resulting in apoptosis [8]. Interestingly, PGRMC2 expression is cell cycle dependent with reduced expression coinciding with entry into the cell cycle [7]. This cell-cycle-dependent change in the expression of PGRMC2 would transiently disrupt or reduce the amount of PGRMC1: PGRMC2 complex and presumably allow for an appropriately timed mitogen-induced entry into the cell cycle.

The mechanism by which the interaction of PGRMC1 and PGRMC2 regulates entry into the cell cycle is not well defined. Our previous studies reveal that PGRMC1 and PGRMC2 bind GTPase activating protein binding protein 2 (G3BP2) and form a complex within the cytoplasm [8]. In addition, depletion of G3BP2 leads to an inappropriate entry into the cell cycle [8]. In HeLa cells, G3BP2 binds the inhibitor of nuclear factor of kappa light polypeptide gene enhancer in B alpha ($I\kappa B\alpha$) and $I\kappa B\alpha$ binds nuclear factor of kappa light polypeptide gene enhancer in B ($\text{NF}\kappa\text{B}$) [9]. These interactions maintain $\text{NF}\kappa\text{B}$'s cytoplasmic localization, thereby inhibiting its transcriptional activity [9].

There are five subunits of $\text{NF}\kappa\text{B}$ that can bind DNA and regulate transcription of genes involved in numerous functions including cell survival and proliferation [10] with $\text{NF}\kappa\text{B}/\text{p}65$ (aka RELA) being highly expressed in ovarian cells [11–14]. $\text{NF}\kappa\text{B}/\text{p}65$ can be activated through a canonical, noncanonical, or atypical pathway [15, 16]. Each of these pathways results in an increase in $I\kappa\text{B}$ kinase (IKK) activity, the phosphorylation and degradation of $I\kappa\text{B}\alpha$, and the translocation of $\text{NF}\kappa\text{B}/\text{p}65$ to the nucleus. Since mitogenic or apoptotic stimuli promote $\text{NF}\kappa\text{B}$ transcriptional activity that leads to the expression of genes involved in cell cycle traverse or apoptosis, respectively [10], it is likely that an intact PGRMC1: PGRMC2: G3BP2 complex functions to restrict entry into the cell cycle by maintaining the $I\kappa\text{B}\alpha$: $\text{NF}\kappa\text{B}$ complex within the cytoplasm.

The present studies were designed to test this hypothesis by first describing the changes in the localization of PGRMC1 and PGRMC2 in nonatretic and atretic follicles within the murine ovaries. A second series of study was then undertaken to determine the effect of granulosa cell specific ablation of *Pgrmc1* on the rate at which granulosa cells enter into the cell cycle and the localization of $\text{NF}\kappa\text{B}/\text{p}65$ in nonatretic and atretic follicles. Finally, studies were designed to assess the functional relationship between PGRMC1, PGRMC2, and $\text{NF}\kappa\text{B}/\text{p}65$ using SIGCs. In these studies, the effect of disrupting the interaction between PGRMC1 and PGRMC2 on the cellular localization of $\text{NF}\kappa\text{B}/\text{p}65$, $\text{NF}\kappa\text{B}$ transcriptional activity, and the rate of entry into the cell cycle was assessed.

Methods and materials

Animals and treatments

All animal procedures were approved by Institutional Animal Care and Use Committee at Washington State University. Three female mice were autopsied at ≈ 4 months of age and the ovaries removed, fixed in 4% paraformaldehyde (PFA), embedded in paraffin, and serially sectioned at $5\ \mu$. These sections were used to localize PGRMC1 and PGRMC2. Briefly, tissue sections were deparaffinized in xylenes, followed by rehydration in decreasing concentrations of ethanol. Endogenous peroxidases were quenched with 10% hydrogen peroxide in methanol. Antigen retrieval was accomplished by boiling in 0.1 M sodium citrate buffer, and slides were cooled to room temperature. Blocking solution containing 2% bovine serum albumin (BSA), 2% normal goat serum, and 0.1% Triton X-100 in phosphate-buffered saline (PBS) was applied for 1 h at room temperature. For the anti-PGRMC1 antibody (Sigma Cat No. SAB2101782), primary antibody was diluted in blocking solution (1:500) and incubated overnight at 4°C . After PBS washes, goat anti-rabbit secondary antibody (Vector, 1:500) was applied for 1 h at room temperature, followed by more PBS washes, and Avidin-Biotin complex (Vector) for 1 h. Slides were washed again with PBS, and DAB substrate was added, followed by hematoxylin stain. When using the mouse monoclonal anti-PGRMC2 antibody (Sigma Cat No. WH001042M4), a complex of primary and secondary antibody was used in order to reduce background resulting from mouse antibody-on-mouse tissue immunostaining. A 1:2000 dilution of anti-mouse secondary antibody (Invitrogen) was incubated for 1 h at 37°C with the anti-PGRMC2 antibody (Sigma, 1:100). Normal mouse serum was added at a 1:2000 dilution and the complex was again incubated at 37°C for 1 h. After blocking for 1 h, this antibody complex was applied to the slides and left on overnight at 4°C . The slides were then rinsed with PBS three times. Avidin-Biotin complex was subsequently added and the protocol continued as for the other antibodies. For the negative control slides, the protocol was identical, except that mouse IgG was added to the complex instead of anti-PGRMC2 antibody.

Conditional knockout mice (*Pgrmc1^{did}*) were used to assess the effect of ablating *Pgrmc1* on follicle growth and atresia. These mice were generated using *Ambr2-cre* mice as described by McCallum et al [17]. For this study, four *Pgrmc1^{fl/fl}* and four *Pgrmc1^{did}* mice at 22–23 days of age were injected with 5-bromo-2'-deoxyuridine (BrdU; i.p. in $100\ \mu\text{l}$ saline; 50 mg/kg body weight). Two hours after injection, the mice were autopsied and the ovaries removed, fixed in 4% PFA, embedded in paraffin, serially sectioned at $5\ \mu$, and used to either assess BrdU incorporation or to localize $\text{NF}\kappa\text{B}$.

To estimate the rate of BrdU incorporation, sections were incubated with an anti-BrdU antibody (Abcam ab152095; diluted 1:100). After 24 h of incubation at 4°C , the slides were then incubated with ImmPRESS peroxidase reagent (Vector Laboratories) for 30 min at room temperature and washed in PBS. The slides were developed using a DAB-peroxidase substrate for 5 min. Finally, the slides were counter stained with hematoxylin for 10 s, rinsed in distilled water, dehydrated, cleared, and mounted. Nuclei that incorporated BrdU were revealed by a dark brown stain. Every fifth section was photographed and using ImageJ software, the color image was converted to a black and white image. The threshold value was adjusted such that only the nuclei detected were those that incorporated BrdU. The area of the granulosa cell layers of each follicle as well as the granulosa cell area that was occupied by BrdU stained cells was determined. The percentage of the granulosa cell area that was occupied by BrdU stained cells for each follicle was calculated and used as

an estimate of the percentage of granulosa cells incorporating BrdU. Follicles were classified according to the following criteria: follicles with 1–2 layers of cuboidal granulosa cells were considered primary follicles (Pedersen Types 3a and 3b); follicles with ≥ 3 layers of granulosa cells but without signs of an antral cavity (Pedersen Types 4, 5a, and 5b) were considered preantral; and any follicles with multiple layers of granulosa cells and an antral cavity were considered to be antral follicles (Pedersen Types 6–8) [18]. Follicles were considered to be atretic if they possessed an oocyte that was not intimately associated with cumulus cells and more than three pyknotic nuclei. The mean percentage of granulosa cells incorporating BrdU ± 1 standard error was calculated for each size class of nonatretic and atretic follicles.

Detection of G3BP2: I κ B α : NF κ B/p65 complexes

SIGCs, which were derived from granulosa cells from rat preovulatory follicles, were maintained in DMEM/F12 supplemented with 5% fetal bovine serum (FBS) [19]. SIGCs were plated at 4×10^5 cells/2 ml of DMEM/F12 with 5% FBS in 35 mm² dishes, which contained a glass cover slip. Lysates for Western blot analysis were made using some of the plates per our previously published protocol [7, 8]. Twenty micrograms of lysate were loaded onto each lane and I κ B α and NF κ B/p65 detected by Western blot analysis using a mouse anti-I κ B α (Cell Signaling Technology Cat #4817) and rabbit anti-NF κ B p65 (Cell Signaling Technology Cat #8242), respectively, following our previously published protocol [7, 8]. Blots in which the primary antibody was omitted served as a negative control to confirm antibody specificity.

Once the antibodies were validated by Western blot analysis, they were used for the immunocytochemical detection of I κ B α and NF κ B/p65. Immunocytochemistry was also used to detect G3BP2 using a rabbit anti-G3BP2 (Assay Biotech Cat # C18193), which was previously validated by Western blot analysis [7]. SIGCs, plated on the glass cover slips, were incubated with an antibody to either G3BP2 (diluted 1: 300), I κ B α (diluted 1:400), or NF κ B/p65 (diluted 1:400) with the primary antibody detected using the appropriate Alexa Fluor 488-labeled secondary antibody. Cells plated on glass cover slips were also used to detect the interaction between I κ B α and either G3BP2 or NF κ B/p65 using the previously cited antibodies in an in situ proximity ligation assay (PLA) [7, 8]. In this protocol, fixed cells were incubated with a mouse antibody to I κ B α and a rabbit antibody to either G3BP2 or NF κ B/p65, depending on which protein–protein interaction was to be investigated. The first antibody incubation was followed by incubation with a pair of oligonucleotide-labeled antibodies: anti-rabbit PLUS and anti-mouse MINUS. These second antibodies were labeled with complimentary DNA oligonucleotides, which under the assay conditions were hybridized and amplified. The interaction between proteins was detected by hybridization of the fluorescent-labeled probe that detected the amplified DNA as a red fluorescent dot. At the completion of this protocol, the cover glass was mounted onto a glass slide using mounting medium, which contained DAPI. As a negative control, one of the primary antibodies was omitted from this protocol.

Effects of disrupting the PGRMC1: PGRMC2 complex or depleting PGRMC1 on NF κ B/p65 localization

SIGCs were plated at 4×10^5 cells in 35 mm² dishes in 2 ml of DMEM/F12 with 5% FBS and cultured for 24 h. To disrupt the interaction between PGRMC1 and PGRMC2, either a goat anti-PGRMC2 antibody (Abcam ab113647) or goat IgG was delivered

into SIGCs using the Chariot transfection reagent (Active Motif, Carlsbad, CA) as previously described [8]. After 3 h of culture, the cells were fixed and NF κ B/p65 detected using a NF κ B/p65 antibody and a secondary antibody labeled with Alexa Fluor 488-labeled anti-rabbit antibody [8]. For each treatment, at least 100 SIGCs were evaluated by sequentially imaging random fields of cells using the GFP filter set to detect NF κ B/p65 and the DAPI filter set to detect the total number of cells (i.e. nuclei). The experiment was repeated three times; the data were pooled and the total number of cells was used to calculate the percentage of cells in which the nuclei were intensely stained for NF κ B/p65.

To assess the effect of reducing the PGRMC1: PGRMC2 complex in vivo, ovarian sections were obtained from the ovaries of the *Pgrmc1*^{fl/fl} control and *Pgrmc1*^{del/del} mice that were used in the BrdU experiment. These sections were stained using the rabbit anti-NF κ B/p65 antibody (diluted 1:800) and the protocol described for BrdU staining. The NF κ B/p65 was revealed by the presence of a brown stain. The percentage of cells with nuclear NF κ B/p65 staining was determined using the counting option in ImageJ. For the smaller follicles, all the granulosa cells in the cross-section were scored for the presence of nuclear NF κ B/p65. For larger preantral and antral follicles, the presence of nuclear NF κ B/p65 was assessed from at least 100 granulosa cells with the cells selected from areas at the ends of the intersecting perpendicular axis of the follicle. Negative controls for each immunohistochemical reaction were conducted by excluding the primary antibody.

NF κ B/p65-dependent transcriptional activity and entry into the cell cycle

Short-interfering RNA treatments

Short-interfering RNAs used to deplete *Pgrmc1*, *Pgrmc2*, and *G3bp2* were purchased from Life Technologies (*Pgrmc1* siRNA ID 25165; *Pgrmc2* siRNA ID168258; *G3bp2* siRNA ID S156617). These siRNAs have been previously tested in SIGCs and shown to reduce their targeted mRNA to $\leq 75\%$ of scramble siRNA controls (AM4611; Life Technologies) after 48 h of culture [8]. To deplete *Nfkb/p65*, siRNA directed against *Nfkb/p65* mRNA was purchased from Cell Signaling Technology (CST #6337) and transfected into cells using lipofectamine 2000 to yield a final concentration of 100 nM. SIGCs were cultured for an additional 48 h. A scramble siRNA (AM4611; Life Technologies) was used as a negative control for all experiments. The effectiveness of the *Nfkb/p65* siRNA treatment was confirmed by real-time PCR using reagents provided by Biosearch Technologies (forward primer: 5'-GAGGCTGTTTGGTTTGAGACATC-3'; reverse primer: 5'-TCTGCCCTCTGACTATCTE-3'; probe: 5'-FAM-CCTTTCTCAAGTGCCTTAATAGCAGGGC-BHQ-1-3'). Values were normalized to *Actb* mRNA levels as previously described [8]. Changes in *Nfkb/p65* siRNA levels after siRNA treatment were expressed as a percentage of the scramble control values.

NF κ B-dependent transcriptional activity

Once the effectiveness of the siRNA treatments was established, SIGCs were plated in 96-well plates in 200 μ l at 8×10^4 cells/well. After 24 h, the cells were transfected with either scramble, *Pgrmc1*, *Pgrmc2*, or *G3bp2* siRNA. Twenty-four hours after siRNA treatment, the cells were transfected with 100 ng of NF κ B -GFP reporter construct (Qiagen Cat # CCS-013G). Experiments also included scramble siRNA-treated cells that were transfected with either the positive or negative control NF κ B reporter constructs. Forty-eight hours after the GFP reporters were transfected, the GFP fluorescence

was monitored using a BioTek Synergy 2 plate reader. The mean negative control value was subtracted from the various siRNA-treated groups and the NF κ B reporter activity expressed as a fold change from scramble siRNA values.

Identification of specific stages of the cell cycle using the FUCCI probe

For these studies, SIGCs were plated and transfected with siRNA as previously described [8]. After 24 h, the cells were infected with Cdt 1-RFP construct (20 viral particles per cell) (ThermoFisher Cat #P36237). The Cdt-RFP construct is one of the FUCCI Cell Cycle Sensor probes that is only expressed in the G₁/early S-phase of the cell cycle [20]. After an additional 24 h of culture, the cells were fixed, stained with DAPI, and images taken of the same field of cells under fluorescent optics using the RFP and DAPI filter sets. The number of cells in the G₁/S-phase (i.e. RFP-stained) and the total number of cells (i.e. DAPI-stained) were counted the percentage of G₁/S-phase cells calculated [5, 7, 8]. Values were expressed as a fold increase in percentage of G₁/S cells.

Statistical analysis

All experiments involving mice include 3–4 *Pgrmc1*^{fl/fl} and 3–4 *Pgrmc1*^{did} mice. For all experiments using SIGCs, treatments were conducted in triplicate or quadruplicate and were replicated a minimum of two times. Values from each experiment were pooled to generate a mean \pm standard error. A Student t-test was used to assess differences between two treatment groups. When comparing more than two groups, a one-way analysis of variance followed by a Fisher's least significant difference post hoc test was used. Data on the percentage of SIGCs with intense NF κ B/p65 nuclear staining were conducted three times; pooled data and the percentage data were analyzed by Fisher exact test. *P* value \leq 0.05 was considered to be significantly different regardless of the statistical test used. All statistical analyses were completed using PRISM software (Version 6.0; GraphPad).

Results

Immunohistochemical studies detected PGRMC1 as a brown stain that was only present when the PGRMC1 antibody was included in the staining protocol (compare Figure 1A with B). Specific staining for PGRMC1 was present throughout the ovary, but the most intense staining was associated with granulosa cells. PGRMC1 localized to the cytoplasm and nucleus of granulosa cells of all sized follicles (Figure 1A, C, E) and follicles in the early stages of atresia showed a localization pattern for PGRMC1 similar to healthy follicles (Figure 1D and E). Only subtle differences were observed in atretic follicles such as more nuclei appeared to be stained for PGRMC1 and PGRMC1 staining in cytoplasmic of granulosa cells was less intense (compare Figure 1E with F).

Like PGRMC1, immunohistochemical analysis detected PGRMC2 as a brown stain that predominately localized to the granulosa cells and this staining was not observed in the negative controls (data not shown). PGRMC2 localized to the cytoplasm of various sized follicles with more intense staining associated with follicles with multiple granulosa cell layers (Figure 2A and B). PGRMC2 retained its cytoplasmic localization in granulosa cells of follicles in the early stages of atresia, although staining intensity in many granulosa cells seemed to be reduced (compare Figure 2B, D with C, E). Taken together, these immunohistochemical studies

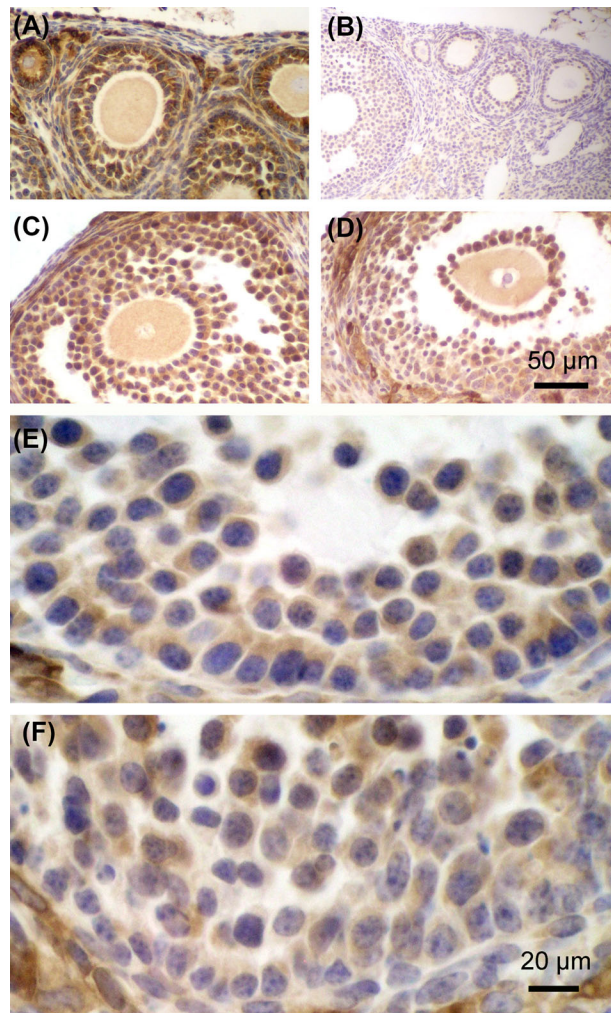


Figure 1. The localization of PGRMC1 within the ovary of an adult mouse. The presence of PGRMC1 is indicated by brown stain in various components of the ovary (A). Note that brown-stained cells are not present in the negative control (B). The granulosa cells of nonatretic primary to preantral follicles (A) and antral (C, E) follicles stain for PGRMC1 in cytoplasm but not all nuclei that are stained blue due to hematoxylin staining. A similar PGRMC1 staining pattern is observed in antral atretic follicles with the most noticeable change being a decrease in PGRMC1 within the cytoplasm and a corresponding increase in nuclear staining (D, F). Images in A–D are taken at the same magnification as shown by the magnification bar in D. Images in E and F are taken at the same magnification shown by the magnification bar in F. A full color version of this figure is available in the online version of this paper.

indicate that the cytoplasmic presence of PGRMC1 and PGRMC2 was diminished in many granulosa cells of follicles in the early stages of atresia while nuclear PGRMC1 staining was increased.

In vitro studies with SIGCs and human granulosa/luteal cells have demonstrated that depletion of either PGRMC1 or PGRMC2 resulted in an inappropriate entry into the cell cycle, which often lead to granulosa cell apoptosis [5, 7]. To determine if PGRMC1 could be depleted within the ovary, *Pgrmc1*^{fl/fl} mice [21] were mated to *Amhr2-cre* mice [17, 22]. This breeding strategy resulted in a 73% reduction in ovarian *Pgrmc1* mRNA compared to controls (*n* = 3/group; *P* = 0.02). It is assumed that this decrease in *Pgrmc1* mRNA was due to a reduction in granulosa cell *Pgrmc1* mRNA as *Amhr2-cre* selectively targets genes that are expressed in the granulosa cells of ovary [22]. Furthermore, PGRMC1 is more

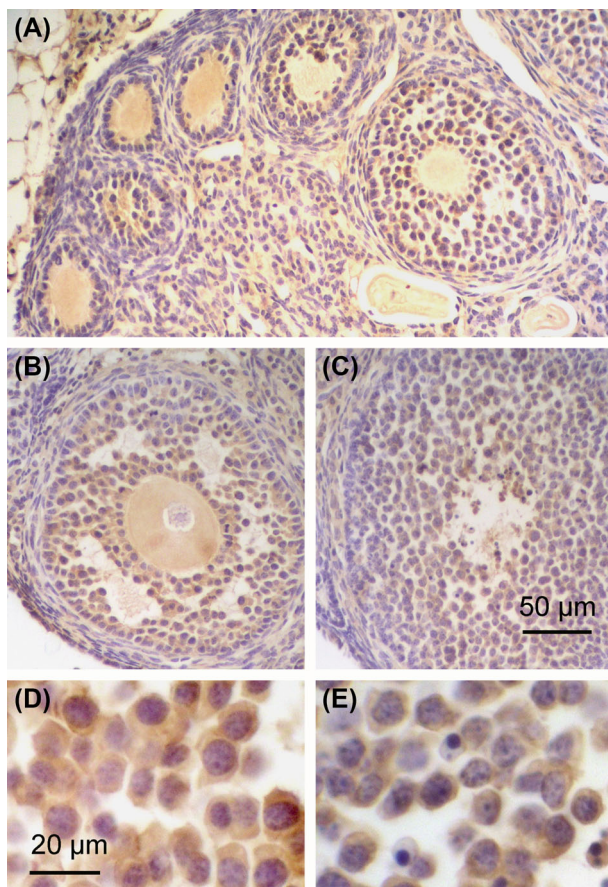


Figure 2. The localization of PGRMC2 within the ovary of an adult mouse. The presence of PGRMC2 is indicated by brown stain in various components of the ovary (A). Note that brown-stained cells were not present in the negative control (data not shown). The granulosa cells of nonatretic primary to preantral follicles (A) and antral (B, D) follicles stain for PGRMC2 mainly in the cytoplasm. A similar PGRMC2 staining pattern is observed in antral atretic follicles with the exception that PGRMC2 staining in some granulosa cells was barely detectable (C, E) with the most noticeable change being a decrease in PGRMC2 within the cytoplasm (E). Images in A–C are taken at the same magnification as shown by the magnification bar in C. Images in D and E are taken at the same magnification shown by the magnification bar in D. A full color version of this figure is available in the online version of this paper.

abundantly expressed in granulosa cells than in the surrounding stromal tissue (Figure 1A).

To determine the involvement of PGRMC1 in regulating follicle growth, BrdU incorporation was used to assess granulosa cell proliferation in *Pgrmc1^{fl/fl}* and *Pgrmc1^{d/d}* immature mice (see Supplemental Figure S1A with B). This study demonstrated that granulosa cells of all sizes of nonatretic follicles from *Pgrmc1^{d/d}* mice entered the cell cycle at a faster rate than those of *Pgrmc1^{fl/fl}* mice as indicated by a 30% increase in the percentage of granulosa cell nuclei that incorporated BrdU within a 2-h time period (Figure 3A, left panel; compare Supplemental Figure S2C with A). Similarly, the percentage of granulosa cells incorporating BrdU in atretic follicles of *Pgrmc1^{d/d}* mice was also elevated compared to atretic follicles of *Pgrmc1^{fl/fl}* mice (Figure 3A, left panel; supplemental Figure S1D with B). While relatively few granulosa cells of atretic follicles of *Pgrmc1^{fl/fl}* mice incorporated BrdU, the rate of BrdU incorporation for granulosa cells of atretic follicles was about three times greater than that observed in the *Pgrmc1^{d/d}* mice (Figure 3C, left panel). Moreover, the percentage

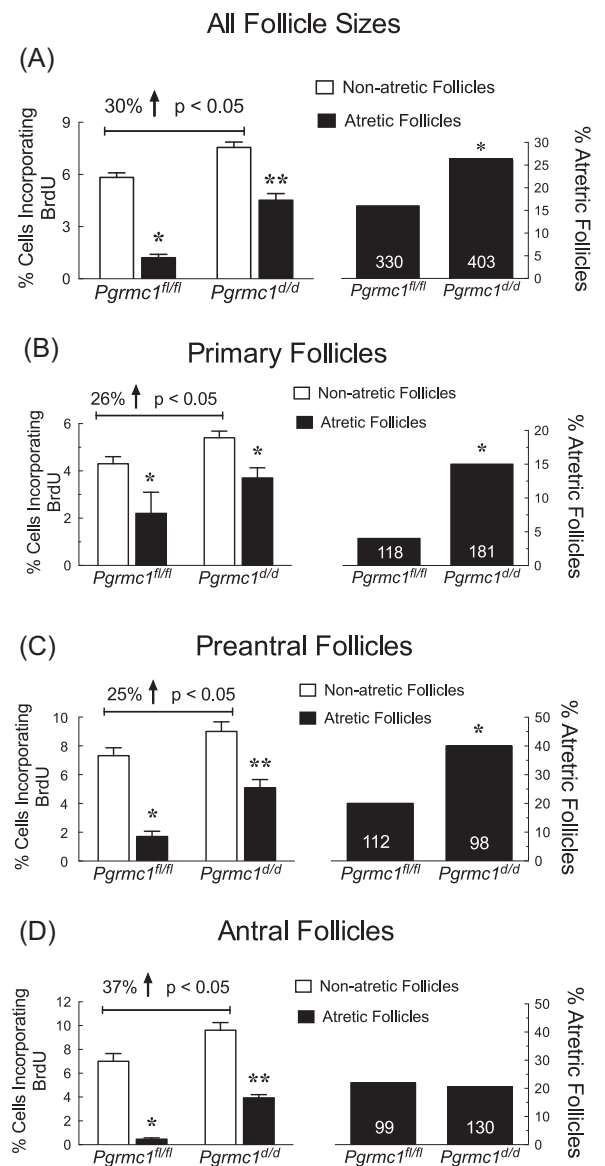


Figure 3. BrdU incorporation in the granulosa cells of nonatretic and atretic follicles of immature *Pgrmc1^{fl/fl}* and *Pgrmc1^{d/d}* mice. The percentage of granulosa cells incorporating BrdU in all sized follicles of *Pgrmc1^{fl/fl}* and *Pgrmc1^{d/d}* mice is shown in A, left panel. The percentage of granulosa cells incorporating BrdU in nonatretic and atretic follicles as well as the percentage of atretic follicles for primary, preantral, and antral follicles is presented in panels B, C, and D, respectively. In this and other graphs, values are presented as means \pm SEM. * indicates a BrdU incorporation value that is different from that of nonatretic follicles of *Pgrmc1^{fl/fl}* mice, while ** indicates a BrdU incorporation value that is different than that of nonatretic follicles of *Pgrmc1^{d/d}* and the atretic follicles of *Pgrmc1^{fl/fl}* mice. The percentage of all sized atretic follicles is shown in A, right panel. * indicates a value greater than *Pgrmc1^{fl/fl}* mice.

of atretic follicles in *Pgrmc1^{d/d}* mice was significantly greater than that of the *Pgrmc1^{fl/fl}* mice (Figure 3C, right panel). As can be seen in Figure 3B–D, these changes in follicular dynamics that are associated with the deletion of *Pgrmc1* from granulosa cells were observed in primary, preantral, and antral follicles, although the percentage of atretic antral follicles in the *Pgrmc1^{d/d}* mice was not different from that of the *Pgrmc1^{fl/fl}* mice.

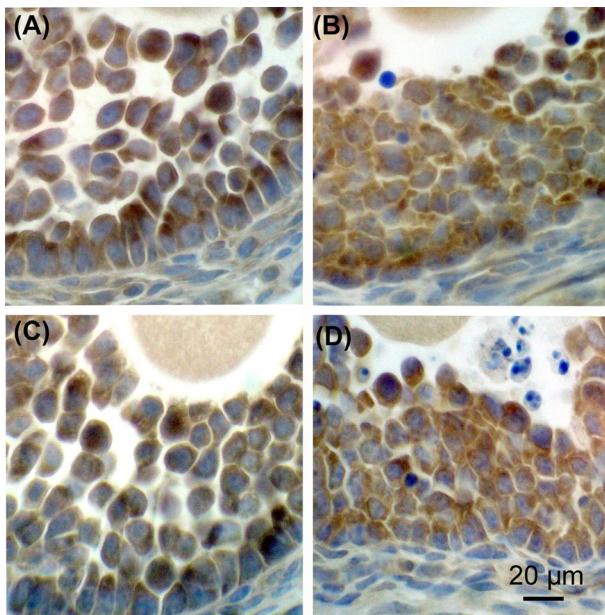


Figure 4. The presence of NF κ B/p65 is indicated by the brown stain in various components of the antral follicles of immature ovaries of *Pgrmc1^{fl/fl}* (A, B) and *Pgrmc1^{d/d}* (C, D) mice. Note that brown-stained cells were not present in the negative control (data not shown). In panel A, a nonatretic antral follicle of a *Pgrmc1^{fl/fl}* mouse is shown in which NF κ B/p65 staining is most intense in the cytoplasm of granulosa cells. In these cells, NF κ B/p65 is detected in $16 \pm 1\%$ ($n = 30$) of nuclei. The nonstained nuclei appeared blue due to the hematoxylin counter stain. Panel B shows an atretic follicle of a *Pgrmc1^{fl/fl}* mouse. In these atretic follicles, NF κ B/p65 staining is more diffuse. In panel C, a small nonatretic antral follicle of a *Pgrmc1^{d/d}* mouse is shown. The NF κ B/p65 staining pattern is similar to that of nonatretic antral follicles of *Pgrmc1^{fl/fl}* mice with the exception that NF κ B/p65 is detected in more granulosa cells nuclei ($25 \pm 1\%$; $n = 30$). This increase in nuclear NF κ B/p65 staining in granulosa cells of nonatretic follicles of *Pgrmc1^{d/d}* mice was observed regardless of follicle sizes. In atretic follicles of *Pgrmc1^{d/d}* mice (D), NF κ B/p65 staining is diffused and detected in both the cytoplasmic and nuclear components of the most granulosa cells similar to that of *Pgrmc1^{fl/fl}* mice (B). A full color version of this figure is available in the online version of this paper.

In granulosa cells from nonatretic follicles of *Pgrmc1^{fl/fl}* mice, NF κ B/p65 staining was typically concentrated within the limited cytoplasm of granulosa cells. This was particularly evident in the granulosa cells underlying the basement membrane of the follicles. In addition, NF κ B/p65 staining was not observed in most of the granulosa cell nuclei, as indicated by the blue hematoxylin staining of most nuclei (Figure 4A). Granulosa cells from nonatretic follicles

of *Pgrmc1^{d/d}* mice showed a similar pattern of NF κ B/p65 staining, although cytoplasmic staining was more diffuse with NF κ B/p65 staining being less pronounced in the granulosa cell layer adjacent to the basement membrane. Moreover, NF κ B/p65 was more frequently detected within the nuclei of granulosa cells from nonatretic follicles of *Pgrmc1^{d/d}* mice (Figure 4C; $25 \pm 1\%$ ($n = 30$)) compared to the granulosa cells from non-atretic follicles of *Pgrmc1^{fl/fl}* mice (Figure 4A; $16 \pm 1\%$ ($n = 30$)) ($P < 0.05$). In granulosa cells of atretic follicles of both *Pgrmc1^{d/d}* (Figure 4D) and *Pgrmc1^{fl/fl}* (Figure 4C) mice, NF κ B/p65 staining was less intense and observed throughout the cell. This was most noticeable in the layer of granulosa cells near the basement membrane of the follicle. Because of the diffuse nature of the NF κ B/p65 staining associated with granulosa cells of atretic follicles, it was difficult to accurately determine the percentage of granulosa cell nuclei that stained for NF κ B/p65, although it appeared that NF κ B/p65 localized to the nuclei of a higher percentage of granulosa cells of *Pgrmc1^{fl/fl}* mice. Similar differences in NF κ B/p65 staining of granulosa cells in nonatretic and atretic follicles were observed in 3-month-old mice (Supplemental Figure S3).

Previous studies have shown that PGRMC1 and PGRMC2 interact with G3BP2. In HeLa cells G3BP2 binds I κ B α which in turn binds NF κ B/p65 thereby limiting NF κ B/p65's cellular localization to the cytoplasm [9]. The present studies were conducted to determine whether similar interactions existed in SIGCs. These studies demonstrated that G3BP2 was detected in the cytoplasm of SIGCs (Figure 5B), confirming previous Western blot and immunocytochemical studies [8]. I κ B α was also expressed by SIGCs as assessed by Western blot analysis (Figure 5A) and immunocytochemistry (Figure 5C). Similarly, NF κ B/p65 was detected in SIGCs as demonstrated by Western blot (Figure 6A) and immunocytochemistry (Figure 5D), consistent with expression of both I κ B α and NF κ B/p65 in mouse granulosa cells [23]. Importantly, PLA revealed that in SIGCs I κ B α interacts with G3BP2 (Figure 5F) and NF κ B/p65 (Figure 5G) with the level of interaction being several times greater than the negative controls (Figure 5E).

Previous work demonstrated that the cytoplasm delivery of a PGRMC2 antibody disrupted the interaction between PGRMC1 and PGRMC2 and resulted in premature entry into the cell cycle [8]. Similarly, depleting G3BP2 triggered an increase in the number of cells entering the cell cycle [8]. This raised that possibility that interfering with the PGRMC1: PGRMC2 interaction could also disrupt the PGRMC: G3BP2: I κ B α : NF κ B/p65 complex and result in NF κ B/p65 entering the nucleus. To test this concept, a PGRMC2 antibody was delivered to the cytoplasm of SIGCs and the percentage of nuclei that stained NF κ B/p65 determined by immunocytochemistry. After exposure to the PGRMC2 antibody, NF κ B/p65 was detected as

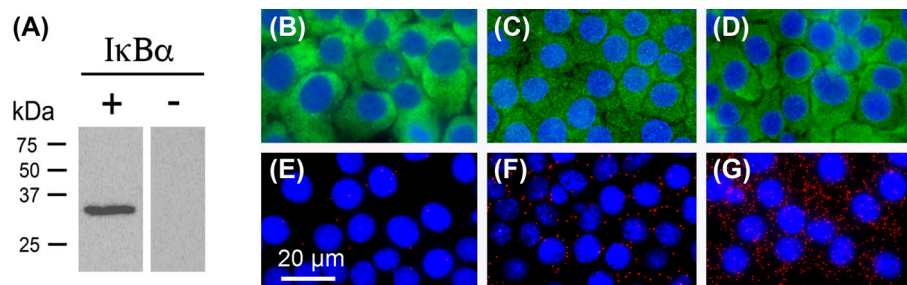


Figure 5. Western blot analysis of I κ B α (+) and a negative control (-) (A). The localization of G3BP2 (B), I κ B α (C), and NF κ B/p65 (C) in SIGCs. A negative control for in situ proximity ligation assay (PLA) has just a few red dots (E). The increase in red dots for the PLAs for G3BP2: I κ B α (F) and I κ B α : NF κ B/p65 (G) indicates their interactions. In panels B, C, and D, the proteins are detected by green fluorescence and nuclei are revealed by blue fluorescence. Negative controls did not detect a green immunofluorescent signal (data not shown). A full color version of this figure is available in the online version of this paper.

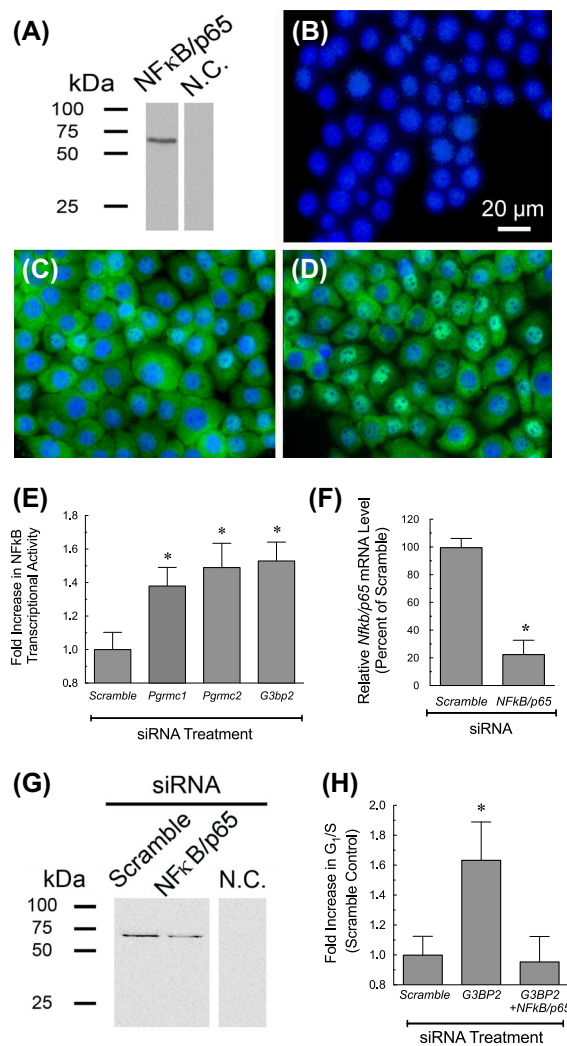


Figure 6. Western blot analysis of NFκB/p65 and a negative control (NC) using SIGC lysates (A). The localization of NFκB/p65 in SIGCs in which either goat IgG (C) or anti-goat PGRMC2 antibody (D) was delivered to the cytoplasm. NFκB/p65 is detected by green fluorescence, and the nuclei stained with DAPI (blue). Note that the distribution of NFκB/p65 was predominately nuclear in the presence of the PGRMC2 antibody. Negative controls did not detect a green immunofluorescent signal (B). The effect of depleting *Pgrmc1*, *Pgrmc2*, and *G3BP2* on NFκB-dependent transcriptional activity as measured using a GFP- NFκB reporter (E). The ability of *NfκB* siRNA to deplete *NfκB/p65* mRNA and protein is shown in panels F and G, respectively. The effect of depleting *NfκB/p65* and/or *G3BP2* mRNA on the percentage of cells entering the cell cycle as judged by using the Cdt-RFP FUCCI probe to detect cells in the G₁/S phase is shown in (H). * indicates a value significantly different from scramble control. A full color version of this figure is available in the online version of this paper.

intense green fluorescent staining in 55% of SIGC nuclei (178 of 322 nuclei) compared to only 6% of those exposed to IgG (18 of 324 nuclei; $P < 0.05$) (compare Figure 6C with D). Note that staining was specific as green fluorescent signal was not detected in the negative controls (Figure 6B).

These immunocytochemical studies demonstrated that disrupting the PGRMC1: PGRMC2 complex either in vitro or in vivo resulted in an increase in nuclear NFκB/p65 and an increased entry into the cell cycle. This implies that these treatments would also increase NFκB transcriptional activity. To test this concept, NFκB

transcriptional activity was monitored in vitro using the GFP- NFκB reporter. As seen in Figure 6E, depleting either *Pgrmc1*, *Pgrmc2*, or *G3bp2* mRNA resulted in a significant increase in NFκB transcriptional activity with the depletion of each component of the PGRMC1: PGRMC2: G3BP2 complex increasing NFκB transcriptional activity to the same degree. To determine whether the increase in NFκB transcriptional activity was responsible for the rapid entry into the cell cycle, *NfκB* siRNA was used. First, an *NfκB* siRNA protocol was developed that resulted in a $\approx 75\%$ decrease in *NfκB* mRNA (Figure 6F) and a corresponding decrease in NFκB protein (Figure 6G). Having established the effectiveness of the *NfκB* siRNA treatment, studies were undertaken to determine whether depleting *G3BP2* could induce entry into the cell cycle in the relative absence of NFκB/p65 using the Cdt-RFP FUCCI probe to detect cells in the G₁/S phase. As shown in Figure 6H, the ability of *G3bp2* siRNA to induce cell cycle entry was dependent of the presence of NFκB/p65.

Discussion

The present studies are the first to examine the localization of PGRMC1 and PGRMC2 in the mouse ovary, and they reveal that both PGRMC1 and PGRMC2 are primarily expressed in the granulosa cells of primary to antral stage follicles. PGRMC1 is present in both the cytoplasm and nucleus of granulosa cells, while PGRMC2 mainly localizes to the cytoplasm. The presence of PGRMC1 and PGRMC2 appears to be reduced in the cytoplasm of many granulosa cells of atretic follicles. These findings are consistent with their localization in the rat ovary [7, 24]. Since PGRMC1 and PGRMC2 promote granulosa cell viability [5, 6, 8, 24], these observations suggest that the reduced levels of PGRMC1 and PGRMC2 could result in granulosa cells undergoing apoptosis with the follicles ultimately becoming atretic and reabsorbed by the interstitial tissue [25].

Support for this concept is based on previous in vitro studies with SIGCs [8, 24] and human granulosa/luteal cells [5, 6]. These studies demonstrate that depleting PGRMC1 or PGRMC2 allows for an inappropriate entry into the cell cycle, which often leads to mitotic arrest and ultimately granulosa cell apoptosis. Further, conditional deletion of *Pgrmc1* from granulosa cells using the *Amhr2-cre* mouse disrupts follicle development. Specifically, conditional deletion of both *Pgrmc1* alleles (*Pgrmc1^{did}*) reduces the number of antral follicles in the ovaries of immature mice by $\approx 50\%$ compared to controls [4]. The ovaries of heterozygous immature mice (*Pgrmc1^{fl/d}*) have the same number of antral follicles as controls but have twice the percentage of atretic antral follicles [4]. It is possible then that depleting both *Pgrmc1* alleles promotes a more rapid demise of granulosa cells, while granulosa cells of the heterozygous mice likely undergo apoptosis at a slower rate. If so, antral follicles undergoing atresia would remain within the ovary of heterozygous mice for a longer period of time than do those of homozygous mice. This would allow for the detection of these atretic follicles and account for the higher incidence of follicle atresia in the heterozygous mouse ovaries. Regardless, these findings from the *Pgrmc1* conditional knockout mouse studies demonstrate that PGRMC1 plays an important role in regulating follicle development in part by regulating granulosa cell cycle progression and survival. It may also explain the tendency for follicles to form ovarian cysts in older *Pgrmc1^{did}* mice [17].

To more precisely define PGRMC1's action, the effect of ablating *Pgrmc1* on the rate of follicle growth was estimated by monitoring the ability of granulosa cells to incorporate BrdU. These studies show that granulosa cells of primary to antral stage follicles of *Pgrmc1^{did}*

mice enter the cell cycle (i.e. incorporate BrdU) more frequently than those of control mice. In addition, the percentage of atretic primary and preantral follicles is $\approx 2\text{--}3$ times greater in the *Pgrmc1^{did}* mice than in control *Pgrmc1^{fl/fl}* mice. However, the percentage of granulosa cells incorporating BrdU in the atretic follicles of *Pgrmc1^{did}* remains elevated. These findings imply that more granulosa cells of small follicles of *Pgrmc1^{did}* mice are entering the cell cycle but are not able to complete mitosis and therefore undergo apoptosis. This fits well with previous in vitro studies in which depletion of *Pgrmc1* results in SIGCs [7] and bovine granulosa cells [26] entering the cell cycle inappropriately, arresting in G₂M stage and subsequently undergoing apoptosis. This type of “mitotic catastrophe” could account for the increase in atresia of primary and preantral follicles observed in the present study, as well as the reduced number of antral follicle in immature *Pgrmc1^{did}* mice [4].

How then does PGRMC1 regulate entry into the cell cycle? Our previous studies reveal that in SIGCs and human granulosa/luteal cells, PGRMC1 forms a complex with PGRMC2 within the cytoplasm and this complex functions to restrict entry into the cell cycle. Moreover, PGRMC2 transiently decreases as cells enter the cell cycle [7]. Although the precise mitotic signal transduction pathway that leads to the transient reduction in PGRMC2 expression is not known, these findings suggest that mitogens decrease the amount of PGRMC2 and thereby the amount of the PGRMC1: PGRMC2 complex. This, in turn, would allow for the controlled entry into mitosis during folliculogenesis, a concept that merits further investigation.

Interestingly, the effect of simultaneously depleting PGRMC1 and PGRMC2 does not increase the rate of entry into the cell cycle over that observed by depleting either PGRMC family member individually [8]. Further, both PGRMC1 and PGRMC2 interact with G3BP2 and form a complex within the cytoplasm [8]. These findings suggest that PGRMC1 and PGRMC2 regulate a common pathway that regulates entry into the cell cycle with one of the common elements in this pathway being G3BP2. Moreover, depleting G3BP2 also results in an inappropriate entry into the cell cycle, thereby supporting this concept [8]. In HeLa cells, G3BP2 has been shown to bind and retain the $\text{I}\kappa\text{B}\alpha$: $\text{NF}\kappa\text{B}$ complex within the cytoplasm, which prevents $\text{NF}\kappa\text{B}$ from translocating to the nucleus [9]. The present studies extend our previous experiments by demonstrating that G3BP2, $\text{I}\kappa\text{B}\alpha$, and $\text{NF}\kappa\text{B/p65}$ not only co-localize but also form a complex within the cytoplasm. Given that G3BP2 also binds PGRMC1 and PGRMC2, it seems likely that a complex composed of PGRMCs, G3BP2, $\text{I}\kappa\text{B}\alpha$, and $\text{NF}\kappa\text{B/p65}$ is present in the cytoplasm of SIGCs and serves to regulate entry into the cell cycle. The present studies with SIGCs demonstrate that, if the interaction between PGRMC1 and PGRMC2 is disrupted, then $\text{NF}\kappa\text{B/p65}$ translocates to the nucleus and drives granulosa cell proliferation. Our studies with *Pgrmc1^{did}* mice further support this concept. These observations imply that an interaction between PGRMC1, PGRMC2, and G3BP2 is required to maintain the cytoplasmic localization of $\text{NF}\kappa\text{B/p65}$. This prevents $\text{NF}\kappa\text{B/p65}$'s translocation to the nucleus and its subsequent transcriptional activity, which is required for entry into the cell cycle. This is supported by the findings that (1) the depletion of G3BP2 increases both $\text{NF}\kappa\text{B}$ transcriptional activity and entry into the cell cycle and (2) the simultaneous depletion of G3BP2 and $\text{NF}\kappa\text{B/p65}$ attenuates the effects of G3BP2 depletion.

The concept that PGRMC: G3BP2 interaction regulates $\text{NF}\kappa\text{B}$ activity by maintaining the $\text{I}\kappa\text{B}\alpha$: $\text{NF}\kappa\text{B/p65}$ complex within the cytoplasm challenges the current concept that an interaction between

$\text{I}\kappa\text{B}\alpha$ and $\text{NF}\kappa\text{B/p65}$ is sufficient to maintain $\text{NF}\kappa\text{B/p65}$'s cytoplasmic location [27]. However, work by Prigent et al. [9] reveals that the N-terminal domain of $\text{I}\kappa\text{B}\alpha$ contains a sequence, referred to as the cytoplasmic retentions sequence, which binds G3BP2 and this interaction is responsible for localizing the $\text{I}\kappa\text{B}\alpha$: $\text{NF}\kappa\text{B/p65}$ complex to the cytoplasm. Moreover, overexpression of G3BP2 retains $\text{I}\kappa\text{B}\alpha$ and $\text{NF}\kappa\text{B/p65}$ in the cytoplasm [9]. The present finding that depletion of G3BP2 results in $\text{NF}\kappa\text{B}$ transcriptional activity supports the concept that $\text{I}\kappa\text{B}\alpha$ is not solely responsible for $\text{NF}\kappa\text{B/p65}$'s cytoplasmic localization and that PGRMC1, PGRMC2, and G3BP2, also regulate $\text{NF}\kappa\text{B/p65}$'s cytoplasmic localization and transcriptional activity. Caution, however, should be exercised in generalizing this conclusion as the role of PGRMC1 and PGRMC2 in regulating G3BP2-dependent $\text{NF}\kappa\text{B}$ transcriptional activity is likely dependent on their level of expression, which is tissue specific. In fact, a stimulatory effect of overexpressing G3BP2 on $\text{NF}\kappa\text{B}$ transcriptional activity was observed in cardiac fibroblasts [28].

The presence of $\text{NF}\kappa\text{B/p65}$ in the PGRMC: G3BP2: $\text{I}\kappa\text{B}\alpha$ complex may be advantageous. For example, G3BP2 is a cytoplasmic protein that does not contain a transmembrane domain (see <https://www.proteinatlas.org/ENSG00000138757-G3BP2/pathology>). Although not essential, anchoring G3BP2 to a membrane could potentially enhance its ability to retain $\text{NF}\kappa\text{B}$ in the cytoplasm. Both PGRMC1 and 2 possess a transmembrane domain [29], which localizes them to the membranes of various cytoplasmic organelles as well as the plasma membrane. Their interaction with G3BP2 could serve to localize $\text{I}\kappa\text{B}\alpha$: $\text{NF}\kappa\text{B/p65}$ complex to specific cellular sites. If the $\text{I}\kappa\text{B}\alpha$: $\text{NF}\kappa\text{B/p65}$ complex resides with a complex that includes PGRMC1, this would potentially bring the EGF receptor into close proximity to $\text{NF}\kappa\text{B/p65}$, since PGRMC1 binds the EGF receptor [30]. Importantly, the activation of the EGF receptor can alter $\text{NF}\kappa\text{B/p65}$'s localization and enhance its activity in part by phosphorylating $\text{I}\kappa\text{B}\alpha$, which results in the degradation of $\text{I}\kappa\text{B}\alpha$ and allows for the entry of $\text{NF}\kappa\text{B/p65}$ into the nucleus [31].

While considerably more studies must be conducted, the previously cited studies suggest that PGRMC1 and PGRMC2 regulate granulosa cell mitosis and apoptosis by controlling $\text{NF}\kappa\text{B/p65}$'s cellular localization and activity. This concept is supported by the findings that FSH-induced follicle growth in mice is dependent in part on FSH's ability to promote the nuclear translocation and DNA-binding activity of $\text{NF}\kappa\text{B}$ [32, 33]. Similarly, a role for $\text{NF}\kappa\text{B}$ in regulating FSH-induced porcine granulosa cell proliferation and survival has been documented [11]. In contrast, progesterone slows the rate of granulosa cell mitosis and enhances granulosa cell viability in vitro [34–37]. In addition, progesterone is most effective in suppressing the rate at which preantral and small antral follicles grow in organ culture [38] and in vivo in response to gonadotropins [39]. Moreover, both the in vitro and in vivo studies suggest that PGRMC1 mediates progesterone's action [38, 39]. These findings are consistent with the present data.

Importantly, the in vivo studies implicate PGRMC1 and its ability to inhibit apoptosis induced by various stressors. Recently, Yuan et al. [39] have shown that exposure to oxidative stressors can induce a rapid increase in $\text{NF}\kappa\text{B}$ activity, which triggers granulosa cell apoptosis and progesterone can counter the effects of stressors in part by inhibiting the phosphorylation and nuclear localization (i.e. activation of $\text{NF}\kappa\text{B}$) with this action being dependent on PGRMC1. Thus, PGRMC1 and PGRMC2 are essential components of the mechanism that regulates $\text{NF}\kappa\text{B/p65}$ in granulosa cells and as such warrant further investigation as $\text{NF}\kappa\text{B/p65}$'s actions are central to our understanding of ovarian function.

Supplementary data

Supplementary data are available at [BIOLRE](https://doi.org/10.1007/s12017-019-0950-0) online.

Supplemental Figure S1. BrdU incorporation in the granulosa cells of immature control (*Pgrmc1^{fl/fl}*) (A) and *Pgrmc1* conditional knockout (*Pgrmc1^{did}*) (B) mice. Images shown in A and B are taken at the same magnification and shown as black and white images with those cells incorporating BrdU shown in a red threshold layer. Note that various sized follicles can be seen in both A and B with amount of BrdU incorporation (Red) being greater in the follicles of *Pgrmc1^{did}* mice (B) compared to those of *Pgrmc1^{fl/fl}* (A).

Supplemental Figure S2. BrdU incorporation as detected by a dark brown-stained nuclei of nonatretic (A, C) and atretic (B, D) follicles within the ovaries of immature *Pgrmc1^{fl/fl}* (A, B) and *Pgrmc1^{did}* (C, D) mice. Sections were counterstained with hematoxylin. All images were taken at the same magnification as shown in the magnification bar in D.

Supplemental Figure S3. Localization of NF κ B/p65 in the adult mouse ovary as detected by a brown stain (A). The negative control taken from an adjacent section is shown in B. Panel C illustrates that NF κ B/p65 localizes to the cytoplasm of various sized follicles prior to antral formation. Panels D and F reveal NF κ B/p65 is mainly concentrated in the cytoplasm, although some nuclear staining is observed. Panel E and G demonstrate that in most granulosa cells of atretic follicles NF κ B/p65 staining is more diffuse with staining detected in most cytoplasmic and nuclear components of the granulosa cells.

References

- Elassar A, Liu X, Scranton V, Wu CA, Peluso JJ. The relationship between follicle development and progesterone receptor membrane component-1 expression in women undergoing in vitro fertilization. *Fertil Steril* 2012; 97:572–578.
- Skiadas CC, Duan S, Correll M, Rubio R, Karaca N, Ginsburg ES, Quackenbush J, Racowsky C. Ovarian reserve status in young women is associated with altered gene expression in membrana granulosa cells. *Mol Hum Reprod* 2012; 18:362–371.
- Mansouri MR, Schuster J, Badhai J, Stattin EL, Losel R, Wehling M, Carlsson B, Hovatta O, Karlstrom PO, Golovleva I, Toniolo D, Bione S et al. Alterations in the expression, structure and function of progesterone receptor membrane component-1 (PGRMC1) in premature ovarian failure. *Hum Mol Genet* 2008; 17:3776–3783.
- Peluso JJ, Pru JK. Non-canonical progesterone signaling in granulosa cell function. *Reproduction* 2014; 147:R169–R178.
- Sueldo C, Liu X, Peluso JJ. Progesterone and AdipoQ Receptor 7, progesterone membrane receptor component 1 (PGRMC1), and PGRMC2 and their role in regulating progesterone's ability to suppress human granulosa/luteal cells from entering into the cell cycle. *Biol Reprod* 2015; 93:1–11.
- Will EA, Liu X, Peluso JJ. AG 205, a progesterone receptor membrane component 1 antagonist, ablates progesterone's ability to block oxidative stress-induced apoptosis of human granulosa/luteal cells. *Biol Reprod* 2017; 96:843–854.
- Griffin D, Liu X, Pru C, Pru JK, Peluso JJ. Expression of progesterone receptor membrane component-2 within the immature rat ovary and its role in regulating mitosis and apoptosis of spontaneously immortalized granulosa cells. *Biol Reprod* 2014; 91:1–11.
- Peluso JJ, Griffin D, Liu X, Horne M. Progesterone receptor membrane component-1 (PGRMC1) and PGRMC-2 interact to suppress entry into the cell cycle in spontaneously immortalized rat granulosa cells. *Biol Reprod* 2014; 91:104–106.
- Prigent M, Barlat I, Langen H, Dargemont C. IkappaBalpha and IkappaBalpha/NF-kappa B complexes are retained in the cytoplasm through interaction with a novel partner, RasGAP SH3-binding protein 2. *J Biol Chem* 2000; 275:36441–36449.
- Riedlinger T, Haas J, Busch J, van de Sluis B, Kracht M, Schmitz ML. The direct and indirect roles of NF-kappaB in cancer: lessons from oncogenic fusion proteins and knock-in mice. *Biomedicines* 2018; 6:1–15.
- Pavlova S, Kluska K, Vasicek D, Korwica J, Sirotkin AV. Transcription factor NF-kappaB (p50/p50, p65/p65) controls porcine ovarian cells functions. *Anim Reprod Sci* 2011; 128:73–84.
- Sirotkin AV. Transcription factors and ovarian functions. *J Cell Physiol* 2010; 225:20–26.
- Sirotkin AV, Alexa R, Kisova G, Harrath AH, Alwasel S, Ovcharenko D, Mlyncek M. MicroRNAs control transcription factor NF-kB (p65) expression in human ovarian cells. *Funct Integr Genomics* 2015; 15:271–275.
- Telleria CM, Goyeneche AA, Stocco CO, Gibori G. Involvement of nuclear factor kappa B in the regulation of rat luteal function: potential roles as survival factor and inhibitor of 20alpha-hydroxysteroid dehydrogenase. *J Mol Endocrinol* 2004; 32:365–383.
- Kaltschmidt B, Greiner JFW, Kadhim HM, Kaltschmidt C. Subunit-specific role of NF-kappaB in cancer. *Biomedicines* 2018; 6:44–56.
- Kendellen MF, Bradford JW, Lawrence CL, Clark KS, Baldwin AS. Canonical and non-canonical NF-kappaB signaling promotes breast cancer tumor-initiating cells. *Oncogene* 2014; 33:1297–1305.
- McCallum ML, Pru CA, Niikura Y, Yee SP, Lydon JP, Peluso JJ, Pru JK. Conditional ablation of progesterone receptor membrane component 1 results in subfertility in the female and development of endometrial cysts. *Endocrinology* 2016; 157:3309–3319.
- Pedersen T. Follicle growth in the mouse ovary. In: Biggers JD, Schuetz AW (eds.), *Oogenesis*. Baltimore, MD: Butterworths; 1972: 397–412.
- Stein LS, Stoica G, Tilley R, Burghardt RC. Rat ovarian granulosa cell culture: a model system for the study of cell-cell communication during multistep transformation. *Cancer Res* 1991; 51:696–706.
- Sakaue-Sawano A, Kurokawa H, Morimura T, Hanyu A, Hama H, Osawa H, Kashiwagi S, Fukami K, Miyata T, Miyoshi H, Imamura T, Ogawa M et al. Visualizing spatiotemporal dynamics of multicellular cell-cycle progression. *Cell* 2008; 132:487–498.
- Clark NC, Pru CA, Yee SP, Lydon JP, Peluso JJ, Pru JK. Conditional ablation of progesterone receptor membrane component 2 causes female premature reproductive senescence. *Endocrinology* 2017; 158: 640–651.
- Jamin SP, Arango NA, Mishina Y, Hanks MC, Behringer RR. Requirement of Bmpr1a for Mullerian duct regression during male sexual development. *Nat Genet* 2002; 32:408–410.
- Son DS, Roby KF, Terranova PF. Tumor necrosis factor-alpha induces serum amyloid A3 in mouse granulosa cells. *Endocrinology* 2004; 145:2245–2252.
- Peluso JJ, Pappalardo A, Losel R, Wehling M. Progesterone membrane receptor component 1 expression in the immature rat ovary and its role in mediating progesterone's antiapoptotic action. *Endocrinology* 2006; 147:3133–3140.
- Familiari G, Vizza E, Miani A, Motta PM. Ultrastructural and functional development of the theca interna. In: Familiari G, Makabe S, Motta PM (eds.), *Ultrastructure of the Ovary*. New York: Springer Science; 1991: 113–128.
- Terzaghi L, Tessaro I, Raucci F, Merico V, Mazzini G, Garagna S, Zuccotti M, Franciosi F, Lodde V. PGRMC1 participates in late events of bovine granulosa cells mitosis and oocyte meiosis. *Cell Cycle* 2016; 15:2019–2032.
- Sakowicz A. The role of NFkappaB in the three stages of pregnancy - implantation, maintenance, and labour: a review article. *BJOG* 2018; 125:1379–1387.
- Hong HQ, Lu J, Fang XL, Zhang YH, Cai Y, Yuan J, Liu PQ, Ye JT. G3BP2 is involved in isoproterenol-induced cardiac hypertrophy through activating the NF-kappaB signaling pathway. *Acta Pharmacol Sin* 2018; 39:184–194.
- Cahill MA. Progesterone receptor membrane component 1: an integrative review. *J Steroid Biochem Mol Biol* 2007; 105:16–36.

30. Ahmed IS, Rohe HJ, Twist KE, Craven RJ. Pgrmc1 (progesterone receptor membrane component 1) associates with epidermal growth factor receptor and regulates erlotinib sensitivity. *J Biol Chem* 2010; **285**:24775–24782.
31. Sun L, Carpenter G. Epidermal growth factor activation of NF-kappaB is mediated through IkappaBalpha degradation and intracellular free calcium. *Oncogene* 1998; **16**:2095–2102.
32. Wang Y, Chan S, Tsang BK. Involvement of inhibitory nuclear factor-kappaB (NFkappaB)-independent NFkappaB activation in the gonadotropic regulation of X-linked inhibitor of apoptosis expression during ovarian follicular development in vitro. *Endocrinology* 2002; **143**:2732–2740.
33. Xiao CW, Asselin E, Tsang BK. Nuclear factor kappaB-mediated induction of Flice-like inhibitory protein prevents tumor necrosis factor alpha-induced apoptosis in rat granulosa cells. *Biol Reprod* 2002; **67**:436–441.
34. Chaffkin LM, Luciano AA, Peluso JJ. Progesterone as an autocrine/paracrine regulator of human granulosa cell proliferation. *J Clin Endocrinol Metab* 1992; **75**:1404–1408.
35. Chaffkin LM, Luciano AA, Peluso JJ. The role of progesterone in regulating human granulosa cell proliferation and differentiation in vitro. *J Clin Endocrinol Metab* 1993; **76**:696–700.
36. Luciano AM, Peluso JJ. Effect of in vivo gonadotropin treatment on the ability of progesterone, estrogen, and cyclic adenosine 5'-monophosphate to inhibit insulin-dependent granulosa cell mitosis in vitro. *Biol Reprod* 1995; **53**:664–669.
37. Peluso JJ, Fernandez G, Pappalardo A, White BA. Membrane-initiated events account for progesterone's ability to regulate intracellular free calcium levels and inhibit rat granulosa cell mitosis. *Biol Reprod* 2002; **67**:379–385.
38. Komatsu K, Masubuchi S. The concentration-dependent effect of progesterone on follicle growth in the mouse ovary. *J Reprod Dev* 2017; **63**:271–277.
39. Yuan XH, Yang CR, Wang XN, Zhang LL, Gao XR, Shi ZY. Progesterone maintains the status of granulosa cells and slows follicle development partly through PGRMC1. *J Cell Physiol* 2019; **234**:709–720.